Properties of transparent PMMA/PEG/MWNTs nanocomposites prepared by in situ polymerizaon

GUOQIN LIU
College of Material Science and Engineering, Henan University of Technology, Zhengzhou, 450001, China

PMMA (poly(methyl methacrylate)) / PEG (poly(ethylene glycol)) / MWNTs (Multi-walled Carbon Nanotubes) (PMMA/PEG/MWNTs) nanocomposites were prepared by in situ polymerization. The effect of different weight percent loadings of MWNTs on the morphological, transmittances and thermal properties of the nanocomposites had been investigated. Scanning electron microscopy (SEM) showed that MWNTs were dispersed uniformly based on the interaction of hydrogen bonds between MWNTs and PEG. When MWNTs were added, the dynamic moduli and thermal stability of PMMA/PEG/MWNTs nanocomposites improved with increasing MWNTs content.

(Received March 9, 2015; accepted March 19, 2015)

Keywords: PMMA/PEG/MWNTs, Nanocomposites, Properties

1. Introduction

Many transparent polymeric materials such as polycarbonate (PC), poly(methyl methacrylate) (PMMA), polystyrene (PS), and poly(vinyl chloride) (PVC) have been widely used in various technological areas including optics and electro-optics, such as optical lenses. In many fields of glazing applications, PMMA is generally chosen as a replacement and currently used extensively, because it has some advantages, for example, good flexibility, high strength, excellent dimensional stability, and so on. However, the current applications of PMMA in optics and electro-optics are limited by their relatively low strength, poor heat resistance, weak mechanical surface, low refractive index, etc[1].

Due to the stronger interactions between polymer and nanofiller phases, in comparison with conventioanl polymer composites, PMMA-based nanocomposites have apparently improved thermal, mechanical and dielectric properties. In the recent years, inorganic nanoparticles (or nanophase materials) have been incorporated into PMMA to overcome its drawbacks. For examples, SiO_2, TiO_2, ZnO, ZrO_2, AlN, Alumina, Calcium carbonate nanoparticles, as well as clay were treated and incorporated into PMMA via in situ polymerization [2-6] or solution blending method [7] to improve the thermal stability of PMMA.

Since carbon nanotubes (CNTs) were discovered, CNTs-based polymer nanocomposites have increasingly drawn more and more attention. CNTs can display a higher aspect ratio and mechanical strength, very high moduli and outstanding electrical properties. The key question of polymer-based nanocomposite in optics and electro-optics application is, when their thermal and mechanical properties are improved, that their transparency have a minimum loss [8-12]. Thus, a lot of researchers have been focusing on the fabrication of strong but transparent polymer nanocomposites [13-17], such as polymethylmethacrylate/cellulose nanocrystals composites, and so on, which showed improvements in both strength and transparency.

In the present study, PMMA networks were prepared and crosslinked by in situ radical bulk polymerization in the presence of PEG and MWNTs via ultrasonic assisting, i.e., PMMA/PEG/MWNTs nanocomposites. In my previous work, blends of linear PEG with PMMA networks are immiscible with PEG > 35 wt % and the PEG crystal can be observed [18]. In order to get transparent PMMA/PEG/MWNTs nanocomposites, PEG content no more than 10 wt % had been utilized to fabricate the nanocomposites. The addition of MWNTs to PMMA/PEG blends may improve the mechanical and thermal properties with little loss in transparency. The effect of different weight percent loadings of MWNTs on the morphological, dynamic mechanical, and thermal properties of PMMA/PEG/MWNTs nanocomposites have been investigated.

2. Experimental

MWNTs (the element of composition (atom%): C: 98.36 , O: 1.30, Al: 0.23, S: 0.05, Fe: 0.06) were supplied from Chengdu Organic Chemicals Co. Ltd., China, with a purity of above 95 %, length:0.5 - 2um, and special surface area: 500 $m^2 \cdot g^{-1}$. The monomer, methyl methacrylate (MMA), was distilled under reduced pressure before use. The radical initiator, 2, 2'-azobis(isobutyronitrile) (AIBN), was recrystallized from ethanol solution. The cross-linker, N,N'-methylenebis(acrylamide) (MBAA) and the hompolymer, PEG with M_w=10000 (Aldrich), which can also play a role of an organic dispersant, were used without further purification.

MWNTs were immersed in 3mol·l^{-1} nitric acid and refluxing for 8 hours, subsequently washed with distilled water until the pH of the MWNTs solution approached 7 and dried at 60 ˚C in a vacuum oven for 24 hours.

0.01, 0.02, 0.03, and 0.04 wt% acid-treated MWNTs (relative to the total amount of MMA monomers, similarly hereinafter.) were separately added into the flask with 10 g of MMA, and 1.0 g of PEG and stirred for 1 hour. Then, the mixtures were sonicated for 30 minutes until MWNTs were finely dispered in it. Subsequently, AIBN (0.1 wt%,) and MBAA (3 wt%,) were added and the flask was purged with N_2 to remove oxygen. The mixtures were sonicated using a bath sonicator for 40 minnutes. Polymerization was carried out with constant stirring at 65 ˚C for 20 minutes. Subsequently, the mixture was injected into the glass plate for for further polymerization at 55 ˚C for 24 hours. The obtained sample was washed several times with ethanol to remove unreacted monomers and dried under vacuum for 4 days at 60 ˚C.

Raman spectra (Renishaw 1000 NR) and Fourier transform infrared spectroscopy (FTIR, Nicolet 200SXV FTIR) were applied for the characterization of raw and acid-treated MWNTs, PMMA/PEG and its nanocomposites. The surface of the gold-coated test sample was observed using Scanning Electron Microscope (SEM, JEOL, JSM-6700F) at an accelerating voltage of 10 kV. Wide-angle X-ray diffraction (WAXD) patterns were obtained using a D8 Advance X-ray diffractometer (Bruker, Germany). The Cu Ka radiation (wavelength = 0.154056 nm) source was operated at 40 kV and 200 mA. WAXD patterns were recorded from 5˚ to 45˚ at 5˚ min^{-1}. Ultraviolet-visible spectra were record with a spectrophotometer (Shimadzu UV spectrophotometer, UV-1800). The dynamic mechanical analyses (DMA, Du Pont 983 DMA) were performed at a fixed oscillation amplitude of 0.1 mm. The frequency of 1 Hz was chosen for all the samples examined. Thermogravimetric analysis (TGA) measurement was performed using TGA-7 (Perkin-Elmer); the sample was heated under air from room temperature to 550 ˚C at a heating rate of 10 ˚C /min.

3. Results and Discussion

The acid-treated CNTs, it is believed, have been covalently linked to some functional groups at their surface, i.e., the formation of the carboxylic acid groups [19, 20]. By the oxidation reaction of MWNTs with the concentrated HNO_3, as a result of an increase in intensity of the disorder band (D-band), the carboxylic acid functionalized MWNTs (MWNTs-COOH) could be characterized by Raman spectra. Raman spectra of raw MWNTs and MWNTs-COOH are presented in Fig. 1.

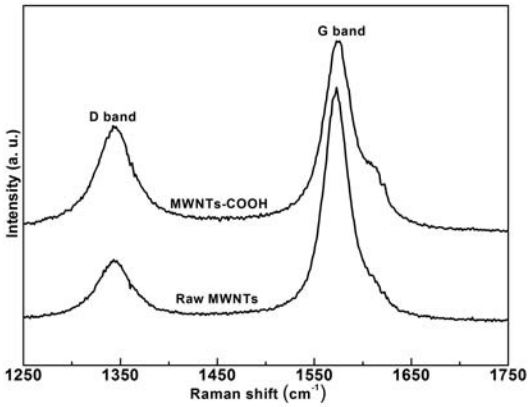

Fig. 1 Raman spectra of raw MWNTs and MWNTs-COOH.

Raman spectroscopy is a very important method for analysis of carbon-based nanostructures, and is to research the presence of amorphous in crystalline phases corresponding to the differences in graphitization, which was comparatively analyzed based on destruction level due to acid treatment process. Both raw MWNTs and MWNTs-COOH have the similar shape in Fig. 1, indicating that after acid-treating, the graphite structure of MWNTs isn't affected. A disorder induced band at 1343 cm^{-1} (D mode) and a strong band at 1574 cm^{-1} (G mode) can be observed. G band reflects the characteristics of graphitic phase owing to in-plane vibration of C atoms which suggests the existence of crystalline graphitic carbon in MWNTs; D band is resulted from disorder induced characteristics such as defects formed in the graphitic planes of MWNTs owing to curvature and existence of amorphous defects in graphite structure. The degree of MWNTs disorder could be evaluated by comparing the I_G/I_D (the characteristic Raman peak ratios) [21]. The I_G/I_D ratio of the prinstine MWNTs and acid-treated MWNTs was 4.36 and 1.92, respectively. This indicates that the acid-treatment increased the degree of disorder of MWNTs and improved the dispersion properties.

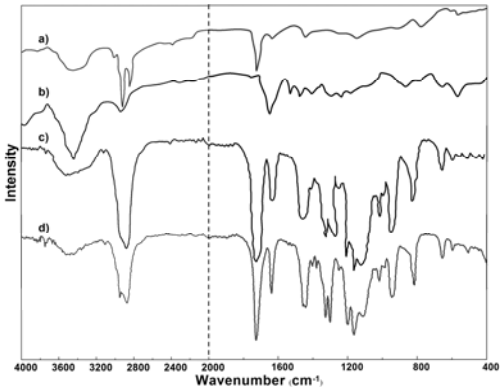

Fig. 2. FTIR spectra of a) MWNTs-COOH,b) raw MWNTs , c) PMMA/PEG/0.04 wt% MWNTs and d) PMMA/PEG.

The interactions between function groups on PMMA/PEG and MWNTs surfaces were characterized by comparing the extent of the shift in absorbing wavelength of key groups in PMMA/PEG and on MWNTs surface after *in situ* radical polymerization. The functional groups of raw MWNTs, MWNTs-COOH, PMMA/PEG and PMMA/PEG/MWNTs from 400 to 4000 cm^{-1} were characterized using FTIR, as shown in Fig. 2. The peaks at 2845, 2918, and 2940 cm^{-1} originate from the stretching vibration of C-H of MWNTs-COOH and raw MWNTs. The hexagonal structure of the pristine MWNTs was in appearance of peak at 1532 cm^{-1} indicating existence of carbon double bonding (C=C) [22]. Decreasing of the C=C absorbance indicates oxidation of carbon with remarkably emergence of peak at 1723 cm^{-1} as carbonyl of carboxyl group, which assigns carbonyl (C=O) stretching vibration of carboxyl groups indicating the expansion of carboxylation on the surfaces of acid-treated MWNTs [23, 24]. Usage of nitric acid in the treatment process causes the improvement of purity as well as partial oxidization of carbon. The number of functional groups should increase after nitric acids oxidation. Acid solution attack double bonding of carbon in decreasing peak region at 1533 cm^{-1} and the hexagonal carbon at region 500 - 1000 cm^{-1}. Reducing the intensity of peak shows presence of large number of asymetrical hexagonal carbon. The sharp peak at 1646 cm^{-1} also assigns to carbonyl of quinone type units along the side walls of the nanotubes which decreased after acid treated. Analysis on quantitative functional groups on the carbon nanotube surface was further evaluated by chemical titration. The above analysis indicate the formation of carboxylic acid groups on the side-walls of the MWNTs.Since there are -COOH groups attached on MWNTs surface, it means the hydrogen bonds are more likely to form between MWNTs-COOH and PMMA/PEG. So, the absorption of -OH group stretching vibrations and -COOH vibration should be paid more attention to, because these groups are most sensitive to hydrogen bonds.

For MWNTs-COOH and PMMA/PEG, as shown in Figure 2, the -OH vibration presents a broad band centered around 3458 and 3495 cm^{-1}. For PMMA/PEG/MWNTs, compared to PMMA/PEG and MWNTs-COOH, the -OH vibration show a broader band centered around 3523 cm^{-1}, which is extremely likely to originate from the formation of hydrogen bonds between PMMA/PEG and MWNTs-COOH. Another region related to hydrogen bond is that of the carbonyl group. For PMMA/PEG and MWNTs-COOH, their C=O vibration appears around 1727 cm^{-1}. Meanwhile, for PMMA/PEG/MWNTs, the frequency of the -C=O stretching is also at 1727 cm^{-1}, however, the -C=O vibration shows a broader band, which means that a weak interaction existed limits the vibrations of some carbonyl groups and the redshift happens. Here, we think the -C=O group of MWNTs-COOH involves in the formation of hydrogen bond, namely, hydrogen bonds existing in between the -C=O of MWNTs-COOH and -OH group of PEG.

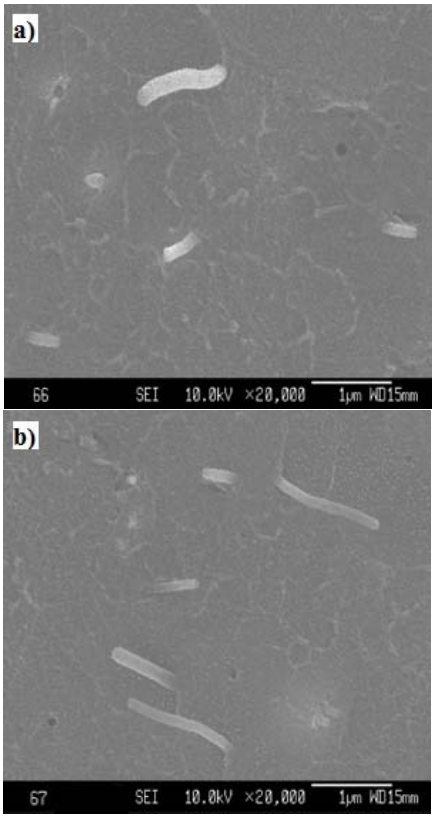

Fig. 3. SEM images of PMMA/PEG/MWNTs nanocomposites. a) PMMA/PEG/0.01 wt% MWNTs; b) PMMA/PEG/0.04 wt% MWNTs.

It is well known that the dispersion of CNTs have an important influence on properties enhancement of polymers/CNTs nanocomposites , such as electrical, mechanical and thermal performances, and so on. The cryo-fractured surface morphology and the state of MWNTs dispersion in the polymer matrix are shown in Fig. 3. However, a good distribution of MWNTs in polymer-based nanocomposites is thought a great challenge because MWNTs have strong tendency to gather and form aggregates [25].

Fig. 3 shows the micrographs of PMMA/PEG/0.01 wt% MWNTs a) and PMMA/PEG/0.05 wt% MWNTs b) nanocomposites. After acid and ultrasonic treatment, MWNTs could be uniformly dispersed. There are some MWNTs detached at one end, while another end still embedded in PMMA/PEG matrix. In Fig. 3, some broken MWNTs are observed, and due to MWNTs high conductivity, their fractured end is shown as some random dispersed bright dots. Those phenomenons can be explained that there exists a interfacial adhesion between MWNTs and PMMA/PEG, which indirectly prove the existence of hydrogen bonds, and the load can be transfered efficiently from PMMA/PEG to MWNTs. The interfacial adhesion usually leads to the significant enhancement of the dynamic mechanical properties [26]. On the other hand, due to a poor interfacial adhesion, some

MWNTs are pulled out of PMMA/PEG matrix and there are some caves (i.e., MWNTs pulled out from PMMA) left on the fractured surface.

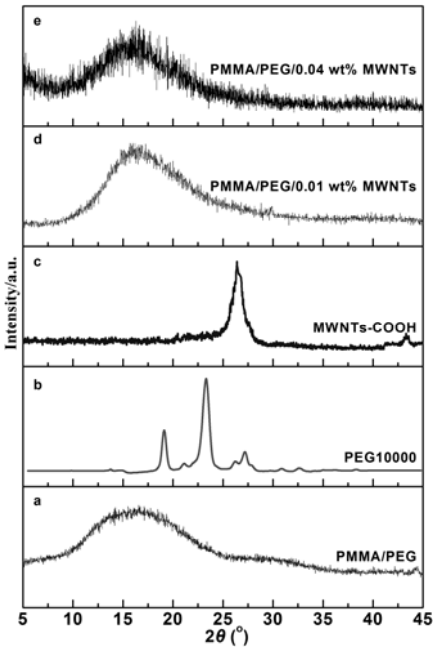

Fig. 4. WAXD patterns of (a) PMMA/PEG, b) PEG10000, (c) MWNTs-COOH, (d) PMMA/PEG/0.01wt% MWNTs and (e) PMMA/PEG/0.04 wt% MWNTs.

It can be also observed that the caves and the bright dots (i.e., the broken MWNTs) embedded in PMMA are well dispersed with no aggregations. It is worth noting the interfaces between the polymeric matrix and MWNTs are very fuzzy, which means that, by HNO_3 treatment, some carboxylic or hydroxylic groups attach on the surface of MWNTs and are in favor of increasing the intermolecular forces or forming hydrogen bonds between MWNTs and PMMA/PEG, improving the dispersion quality of MWNTs, and decreasing the formation of severe MWNTs aggregations. Meanwhile, there are some MWNTs having a diameter of over 100 nm, while in the case of raw MWNTs, their diameter is generally about 70 nm, which means that MWNTs might coated with the polymer matrix via *in situ* polymerization, thereby improving the compatibility of MWNTs and polymer. Thus, the uniform distribution of MWNTs is clearly observed in PMMA/PEG, as shown in Fig. 3.

There exists a crystalline phase in PMMA/PEG with PEG > 35 wt % and the PEG crystal can be observed [18]. To prepare transparent PMMA/PEG/MWNTs nanocomposites, the content of PEG is controlled no more than 10 wt %. However, MWNTs are generally thought to act as a nucleating agent [27, 28]. Thus, whether the incorporation of MWNTs induces the crystallization of PEG in PMMA/PEG/MWNTs nanocomposites is very important for the fabrication of transparent PMMA/PEG/MWNTs nanocomposites.

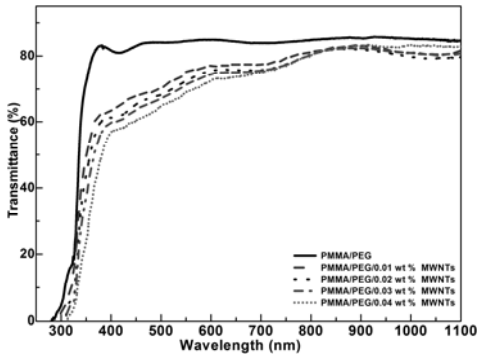

Fig. 5. Transmittance UV-vis spectra of PMMA/PEG and PMMA/PEG/MWNTs nanocomposites.

The WAXD patterns of MWNTs-COOH, PEG10000, PMMA/PEG and its nanocomposites are shown in Fig. 4. All samples were cooled at 25 ˚C for 8 hours. The XRD pattern of the PMMA/PEG shows a broad peak at 16˚, confirmed the amorphous feature of the PMMA/PEG blends. For the PEG10000, the two distinct reflection peaks centered at 2θ of 19˚ and 23˚ correspond separately to the (120) and (132) reflections of PEG monoclinic unit cell [29-31]. Compared with WAXD patterns of PEG1000 homopolymer, the two characteristic diffraction peaks mentioned above disappear in PMMA/PEG, which indicates that there are good compatibility between PMMA and PEG. Meanwhile, MWNTs-COOH displays the diffraction peaks at 26˚ and 43˚, corresponding to the hexagonal graphite structures (002) and (100), respectively [32]. Although MWNTs could act as a nucleating agent in many polymer systems, in the PMMA/PEG/MWNTs nanocomposites, the two characteristic diffraction peaks related to PEG crystalline cannot be observed and the XRD pattern of the nanocomposites exhibits the similar to that of observed from the PMMA/PEG matrix, suggesting that no crystalline phase had been introduced into the nanocomposites. In other words, the addition of MWNTs into PMMA/PEG doesn't induce the crystallization of PEG in the nanocomposites. Likewise, the characteristic diffraction peaks of MWNTs also disappear in the nanocomposites; this result indicates that a very thin polymer layer is very likely to be coated on the surface of MWNTs, which is in agreement with the SEM analysis discussed above.

The transparencncy of PMMA/PEG/MWNTs nanocomposites is very important for its application in optics and electro-optics. The information concerning the transparency of the nanocomposites and the uniformity of MWNTs dispersion can be quantitatively obtained from the UV-vis spectra. Fig. 5 shows the the UV-vis spectra of all four nanocomposites displayed a transmittance of 50% and higher at or above 380 nm, which reveals a strong absorption probability below 380 nm. In contrast, for PMMA/PEG blends, they show the high transmittance than the other nanocomposites; their percent transmittances at 400, 500, and 600 nm are 82%, 84%, and 85%, respectively. While PMMA/PEG with 0.01, 0.02,

0.03 and 0.04 wt% of MWNTs, those of transmittances are 77%, 76%, 74%, and 72%. The prepared PMMA/PEG/MWNTs nanocomposites have high transparency near IR spectral region and, for PMMA/PEG//0.04 wt% MWNTs nanocomposites, the transparency reaches up to 83.3% at 1000 nm. It should be emphasized that the incorporation of MWNTs into polymer decreases more or less the transparency of PMMA. On the other hand, the higher transparency means that MWNTs can't act as a nucleating agent inducing PEG to crystallize and are well dispersed, which are consistent with the above analysis.

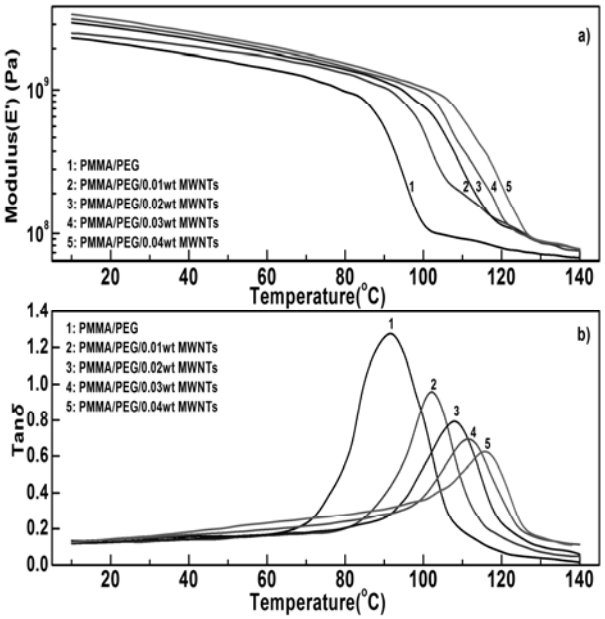

Fig. 6 Dynamic mechanical results for PMMA/PEG and PMMA/PEG/MWNTs nanocomposites: a) storage modulus (E') and b) loss factor (tanδ) versus temperature.

Fig. 6 a) and b) show the DMA curves of PMMA/PEG and PMMA/PEG/MWNTs nanocomposites with 0.5, 0.75, 1 and 1.5 wt% of MWNTs. The storage modulus (E´) can express the stiffness of visco-elastic materials and is proportional to the energy stored. At low temperatures, macromolecular motions are 'frozen' and restricted resonating with the oscillatory loads, which makes polymer's rigidity enhance. The movements of macromolecular segments are restricted with no location change, especially through rotation about C–C bonds, and so the macromolecular entanglements could act as a physical crosslinking. At elevated temperatures, the macromolecular chains can move more and more freely. The slipping and disentanglement of macromoleculars may sometimes happen, although their entanglements still remain firmly in place. The addition of MWNTs shows a increase in E' of PMMA/PEG blends, resulted from less free space for macromoleculars vibration in the presence of MWNTs. The vast interfacial area created by well-dispersed MWNTs can affect the behaviour of the surrounding polymer matrix, creating a co-continuous network of dramatically altered polymer chains movement, and fundamentally changing the mechanical and thermal properties of the matrix [33, 34].

In Fig. 6 a), PMMA/PEG shows a value of $E' = 2.27$ GPa at 10 ˚C; while PMMA/PEG with 0.01, 0.02, 0.03 and 0.04 wt% of MWNTs, the values of E' are 2.45, 2.90, 3.07 and 3.31 GPa. However, the respective E' values are 056, 1.04, 1.14, 1.21 and 1.27 GPa at 90 ˚C. These results show a relevant rise in PMMA/PEG/MWNTs nanocomposites and represent an increment in E' of at least 18.4 % with respect to PMMA/PEG matrix at 20 ˚C. When MWNTs are added into polymers, it seems that MWNTs play an important role in the effective immobilization of the macromoleculars chains motion. So, PMMA/PEG/MWNTs nanocomposites show higher E' values. The average glassy-state modulus of PMMA/PEG/MWNTs nanocomposites increases with increasing MWNTs content, resulting from the superior interfacial bonding and the persistently good dispersion of MWNTs. With increasing of MWNTs content, they increases the modulus by not only their own stiffness but also the new-generated 'inter-phase' stiffness. At 90 ˚C the E' of PMMA/PEG/MWNTs nanocomposites is higher at least more than 1.86-fold in contrast with PMMA/PEG blends.

The glass transition temperatures (T_g) can be observed from the curves of loss factor (tanδ) in DMA. T_g values are taken from the peak of the tanδ curves. Fig. 6 b) shows tanδ as a function of temperature. Due to their smaller size, higher surface area, and greater surface roughness, MWNTs can strongly adsorb the macromolecules of the nanocomposites, restricting macromolecular movement. Thus, T_g of the nanocomposites increases with increasing of MWNTs content. Taking the T_g of PMMA/PEG blends as a contrast, MWNTs can increase the T_g of the nanocomposites by at least as much as 10 ˚C.

The increasing of Tg in the nanocomposites means that MWNTs well disperse in polymer matrix, and a vast interfacial area of MWNTs alters polymer chain mobility throughout the nanocomposites. This consistent interaction between PMMA/PEG blends and MWNTs reduces the polymer macromolucular movement. Thus, the interfacial area between polymer and MWNTs enlarges with increasing of MWNTs content, making an increase in T_g as well as more increases in modulus. On the other hand, tanδ represents the energy lost and the mechanical damping or internal friction in a viscoelastic system. Tanδ is expressed as a dimensionless number. The higher the tanδ, the more nonelastic strain the material. However, a low tanδ value indicates that a material has a more elastic component. This may be attributed to MWNTs acting as physical cross-links, which partially restrict macromolecular movements, increase the stiffness of PMMA/PEG/MWNTs nanocomposites, and are reversible.

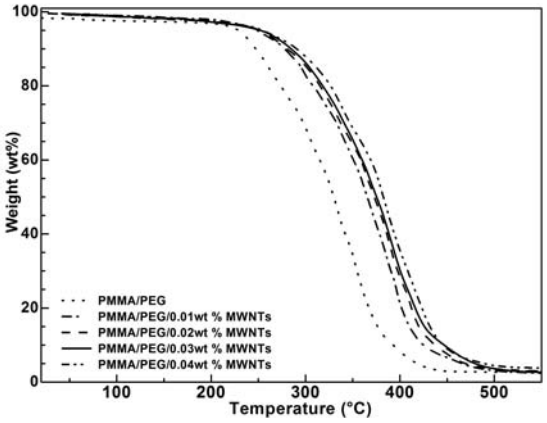

Fig. 7. TGA curves of PMMA/PEG and PMMA/PEG/MWNTs nanocomposites.

Thermogravimetric analysis can evaluate the thermal stabilities of PMMA/PEG and PMMA/PEG/MWNTs nanocomposites. Fig. 7 shows that the onset degradation temperature (T_d, 5% weight loss temperature) of PMMA/PEG is at least ca. 20 C˚ lower than that of PMMA/PEG/MWNTs nanocomposites. MWNTs delay the thermal degradation of the resulting nanocomposites. The homogeneously distributed MWNTs could prevent the emission of thermally degraded small gaseous molecules, slowing thermal degradation of the nanocomposites are much slower compared with PMMA/PEG. Besides that, the residual weight of PMMA/PEG/MWNTs nanocomposites left increases steadily with the increase of MWNTs loading. As shown in Figure 8, the weight loss at 374 ˚C for PMMA/PEG is about 85%, whereas PMMA/PEG/MWNTs nanocomposites are only around 44–58%. This also indicates that the thermal stability of PMMA/PEG is improved on incorporation of MWNTs.

4. Conclusions

PMMA/PEG/MWNTs nanocomposites were prepared via in situ polymerization with 0.01; 0.02; 0.03 and 0.04 wt% of MWNTs content. Based on the interaction of hydrogen bonds between MWNTs and PEG, MWNTs could be uniformly distributed in PMMA/PEG matrix without any aggregates. Although MWNTs could act as a nucleating agent, they don't induce the crystallization of PEG in the nanocomposites. PMMA/PEG/MWNTs nanocomposites have an increment in elastic modulus of at least 18.4 % at 20 ˚C, and are higher at least more than 1.86-fold at 90 ˚C. DMA tests also shows that the incorporation of MWNTs into PMMA/PEG clearly increases the nanocomposites's T_g more than 10 ˚C and PMMA/PEG/MWNTs nanocomposites becomes more elastic as more MWNTs are added. TGA results indicate that the addition of MWNTs into PMMA/PEG blends improves the thermal stability of the polymer matrix.

Reference

[1] Y. Hu, S. Zhou, L. Wu, Polymer **50**, 3609 (2009).
[2] A. H. Yuwono, B. Liu, J. Xue, J. Wang, H. I. Elim, W. Ji, Y. Li, T. J. White, J. Mater. Chem. **14**, 2978 (2004).
[3] A. H. Yuwono, J. Wang, H. I. Elim, W. Ji, Y. Li, T. J. White, J. Mater. Chem. **13**, 1475 (2003).
[4] H. Althues, R. Palkovits, A. Rumplecker, P. Simon, W. Sigle, M. Bredol, U. Kynast, S. Kaskel, Chem. Mater. **18**, 1068 (2006).
[5] S. Li, M. S. Toprak, Y. S. Jo, J. Dobson, D. K. Kim, M. Muhammed, Adv. Mater. **19**, 4347 (2007).
[6] R. T. Chai, H. Z. Lian, P. P. Yang, Y. Fan, Z. Y. Hou, X. J. Kang, J. Lin, J. Colloid Interf. Sci. **336**, 46 (2009).
[7] M. M. Demir, P. Castignolles, U. Akbey, G. Wegner, Macromolecules **40**, 4190 (2007).
[8] Z. Jin, K. P. Pramoda, G. Xu, S. H. Goh, Chem. Phys. Lett. **337**, 43 (2001).
[8] C. Park, Z. Ounaies, K. A. Watson, R. E. Crooks, J. S. Jr, S. E. Lowther, J. W. Connell, E. J. Siochi, J. S. Harrison, T. L. St Clair, Chem. Phys. Lett. **364**, 303 (2002).
[9] G. M. Odegard, T. S. Gates, K. E. Wise, C. Park, E. J. Siochi, Compos. Sci. Technol. **63**, 1671 (2003).
[10] Z. Ounaies, C. Park, K. E. Wise, E. J. Siochi, J. S. Harrison, Compos. Sci. Technol. **63**, 1637 (2003).
[11] L.M. Clayton, A.K. Sikder, A. Kumar, M. Cinke, M. Meyyappan, T. G. Gerasimov, J.P. Harmon, Adv. Funct. Mater. **15**, 101 (2005).
[12] H. Liu, D. Liu, F. Yao, Q. Wu, Bioresource Technol. **101**, 5685 (2010).
[13] Y. Shimazaki, Y. Miyazaki, Y. Takezawa, M. Nogi, K. Abe, S. Ifuku, H. Yano, Biomacromolecules **8**, 2976 (2007).
[14] M. Nogi, K. Handa, A. N. Nakagaito, H. Yano, Appl. Phys. Lett. **87**, 243110 (2005).
[15] M. Nogi, S. Ifuku, K. Abe, K. Handa, A. N. Nakagaito, H. Yano, Appl. Phys. Lett. **88**, 133124 (2006).
[16] D. Blond, V. Barron, M. Ruether, K. P. Ryan, V. Nicolosi, W. J. Blau, J. N. Coleman, E. J. Siochi, J. S. Harrison, Adv. Funct. Mater. **16**, 1608 (2006).
[17] Y. Li, Q. Ma, C. Huag, G. Liu, Mater. Sci-Medzg. **19**, 147 (2013).
[18] H. Hu, P. Bhowmik, B. Zhao, M. A. Hamon, M. E. Itkis, R. C. Haddon, Chem. Phys. Lett. **25**, 345 (2001).
[19] H. Hu, B. Zhao, M. E. Itkis, R. C. Haddon, J. Phys. Chem. B **107**, 13838 (2003).
[20] J. Zeng, B. Saltysiak, WS. Johnson, DA. Schiraldi, S. Kumar, Compos. Part B-Eng. 35, **173** (2004).
[21] M. Vesali Naseh, A. A. Khodadadi, Y. Mortazavi, O. Alizadeh Sahraei, F. Pourfayaz, S. Mosadegh Sedghi, World Acad. Sci. Eng. Technol. **49**, 177 (2009).

[22] S. Chen, W. Shen, G. Wu, D. Chen, M. Jiang, Chem. Phys. Lett. **402**, 302 (2005).
[23] S. Y. Lee, S. J. Park, B. Korean Chem. Soc. **31**, 1596 (2010).
[24] P. M. Ajayan, L. S. Schandler, C. Giannaris, A. Rubio, Adv. Mater. **12**, 750 (2000).
[25] D. Chen, M. Wang, W. D. Zhang, T. Liu, J. Appl. Polym. Sci. **113**, 644 (2009).
[26] R. A. Perez, J. V. Lopez, Macromolecules **47**, 3553 (2014).
[27] H.Fang, F. Wu, J. Appl. Polym. Sci. **131**, 40849 (2014).
[28] H. Tadokoro, Y. Chatani, T. Yoshihara, S. Tahara, S. Murahashi, Makromol. Chem. **73**, 109 (1964).
[29] Y. Takahashi, I. Sumita, H. J. Tadokoro, Polym. Sci., Polym. Phys. Ed. **11**, 2113 (1973).
[30] Y. Takahashi, H. Tadokoro, Macromolecules **6**, 672 (1973).
[31] W. Li, C. Liang, W. Zhou, J. Qiu, Z. Zhou, G. Sun, Q. Xin, J. Phys. Chem. B **107**, 6292 (2003).
[32] S. T. Kim, H. J. Choi, S. M. Hong, Colloid Polym. Sci. **285**, 593 (2007).
[33] Y. Zhao, Z. Qiu, W. Yang, J. Phys. Chem. B **112**, 16461 (2008).

*Corresponding author: polymerpaper@163.com